CHAPTER VII

RESULTS, ANALYSIS AND MODEL VALIDATION

7.1 INTRODUCTION

Several theoretical models, as described in Chapter 4, were considered and field experiments undertaken (Chapters 5 and 6). In this Chapter, the results of the theoretical modelling and the field experiments will be discussed and the models validated. The findings will be analyzed.

7.2 THE DISTRIBUTION OF CONTACT PRESSURE

The analysis by several researchers (Wills, 1963; Wong, 1993) proved that the contact pressure distribution affects the development of tractive effort. For both wheels and tracks the prediction of the contact pressure distribution is of vital importance in analytical traction modelling.

By applying the equations and procedures as discussed in Chapter 4, the distribution of the ground contact pressure can be predicted.

The sinkage of any point at the contact surface was determined by the assumed configuration of the track deformation as shown in Figure 4.2 (p 4-8) for the idealized distribution and Figure 4.4 (p 4-13) for the flexible deformation. By using the Bekker's sinkage equation [equation (2.1), p 2-5], the sinkage was calculated by equations (7.2) and (7.3) on page 4-14 for front and rear wheels respectively in the flexible model. Then the equation (2.1) was used to calculate the pressure at any point from sinkage and the related soil sinkage parameters. Therefore the distribution of the contact pressure below the track was predicted.

For hard surface, because it was impossible to measure and apply the relationship of sinkage and contact pressure, the distribution of contact pressure and also the distribution of tangential friction stress were not predicted.

The comparison between the measured contact pressure distribution and the predicted values, based on the flexible track model, will be discussed.

7.2.1 The contact pressure distribution and frictional stress on a hard surface

For the calculation of the actual rolling radius of the track, a test run on a concrete surface without drawbar load was undertaken. During this test, the contact pressure and the horizontal force on the track element were measured. Figure 7.1 shows the curves for the measured contact pressure distribution as well as the frictional stress.

From the figure, it is clear that the contact pressure distribution for a hard surface varies considerably over the longitudinal span of the track. However, the measured results also proved that the contact pressure distribution for the prototype track differs from the load distribution pattern for the case of wheel tractors. The section of the track only in contact with the road surface carries part of the vertical load. In this regard, the prototype track changes the pattern of contact pressure distribution by reducing the peak values of the pressure below both the front and the rear ends of the track.

By summation of the horizontal force components for each track element at zero drawbar pull, the total rolling resistance for one track was obtained as 8.0 kN. Therefore, the total rolling resistance on concrete road, when the tractor was self-propelled, was 16.1 kN for two tracks. On the other hand, with the free rolling tractor in neutral was pulled by another tractor, the pulling force was measured as 9.5 kN. Therefore the motion resistance on concrete surface was accepted as 12.8 kN which was the average of the above two rolling resistance values.

Based on the measured curves of the contact pressure distribution as shown in Figure 7.1, it is seen that the expected soil entry effect for a soft terrain surface did not occur in the case of driving on the hard surface. It was expected that the peak values of the contact pressure would have occurred below the centres of the front and the rear axles. However, the peak value of the contact pressure for the front axle was slightly behind the axle centre of the front wheels, probably due to lack of the entry effect.

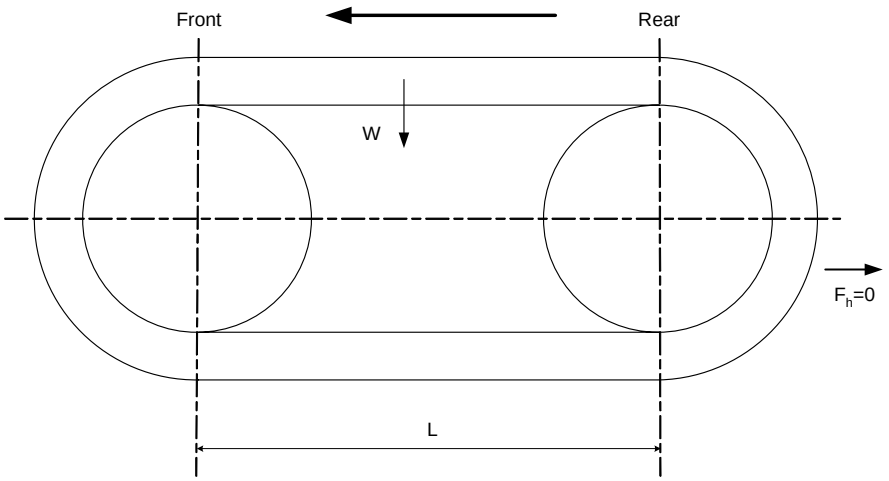

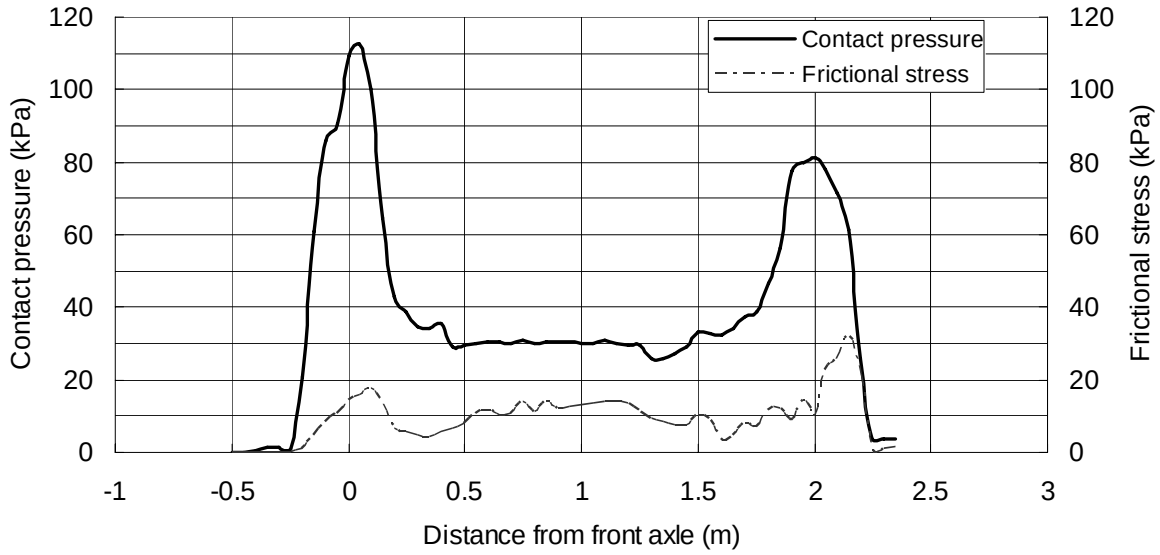

Figure 7.1. The measured distribution of contact pressure and frictional stress on concrete surface (drawbar pull=0).

7.2.2 The effect of the ground wheels on the pressure distribution and frictional stress for a hard surface

The measured contact pressure distribution and frictional stress on a concrete surface, with the centre wheels pushed down onto the track and thus road, is shown in Figure 7.2.

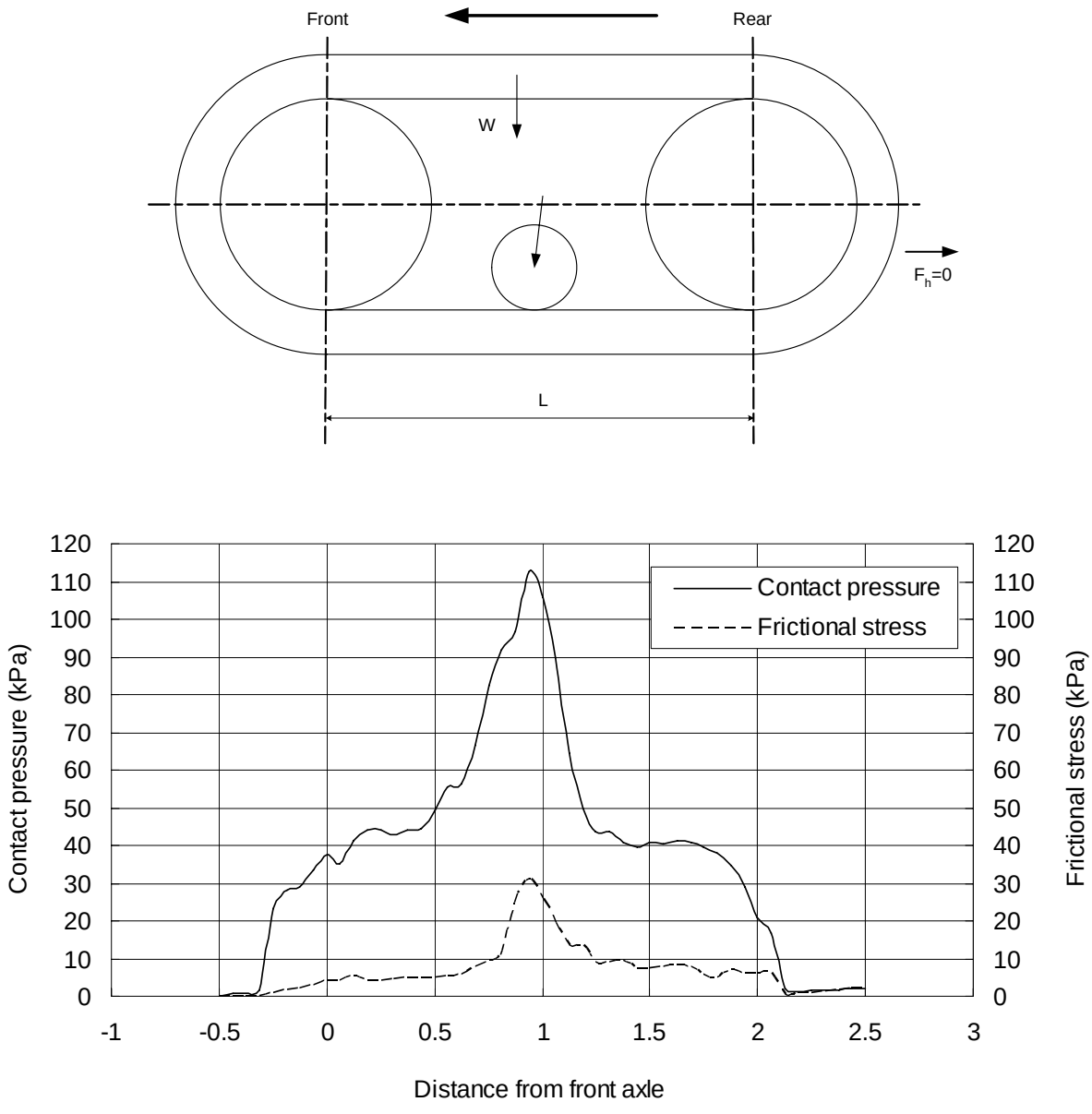

Figure 7.2. The measured contact pressure distribution and frictional stress on a concrete surface when the ground wheels in the middle of the track were pushed down (drawbar pull = 0).

As described in the previous Chapters, the originally planned function of the centre ground wheels were to reduce steering resistance, the skidding effect and soil surface damage which occurred for the traditional steel track design when the tractor was steered. It proved that the middle wheels carried a large portion of the vertical load and a high peak value of contact pressure appeared directly below the loading point of the middle wheels.

For the load wheels forced down, the rolling resistance for the tractor was measured as 15.9 kN, based on the summation of the horizontal force components. It therefore depicted a slightly reduced value when compared to the case when the middle wheels were not used.

During the field test, the operator tried to control the load on the middle wheels within a moderate range in order to obtain a more uniform contact pressure distribution. However, with the manual control, it was rather difficult to keep the pressure at a desired level.

A hydraulic close loop control system could be considered for future improved pressure control. The hydraulic pressure could be used as feedback signal.

7.2.3 The contact pressure distribution and frictional stress on a soft surface with zero drawbar pull

The established model could be used to predict the contact pressure distribution on soft terrain surface after the relevant soil characteristics based on the bevameter technique were obtained. Figure 7.3 shows the predicted distribution of the contact pressure and frictional stress as well as the measured contact pressure and frictional stress.

Equations (4.19) and (4.20) on page 4-14 were applied to calculate the sinkage for front and rear wheels respectively. Then the contact pressure at any point below the

track was calculated by the pressure-sinkage relationship as expressed by equation (2.1) (p 2-5) after the sinkage of any point at the contact surface was determined by the assumed profile configuration of the track deformation as shown in Figure 4.4 (p 4-13). The distribution of the contact pressure below the track was therefore predicted.

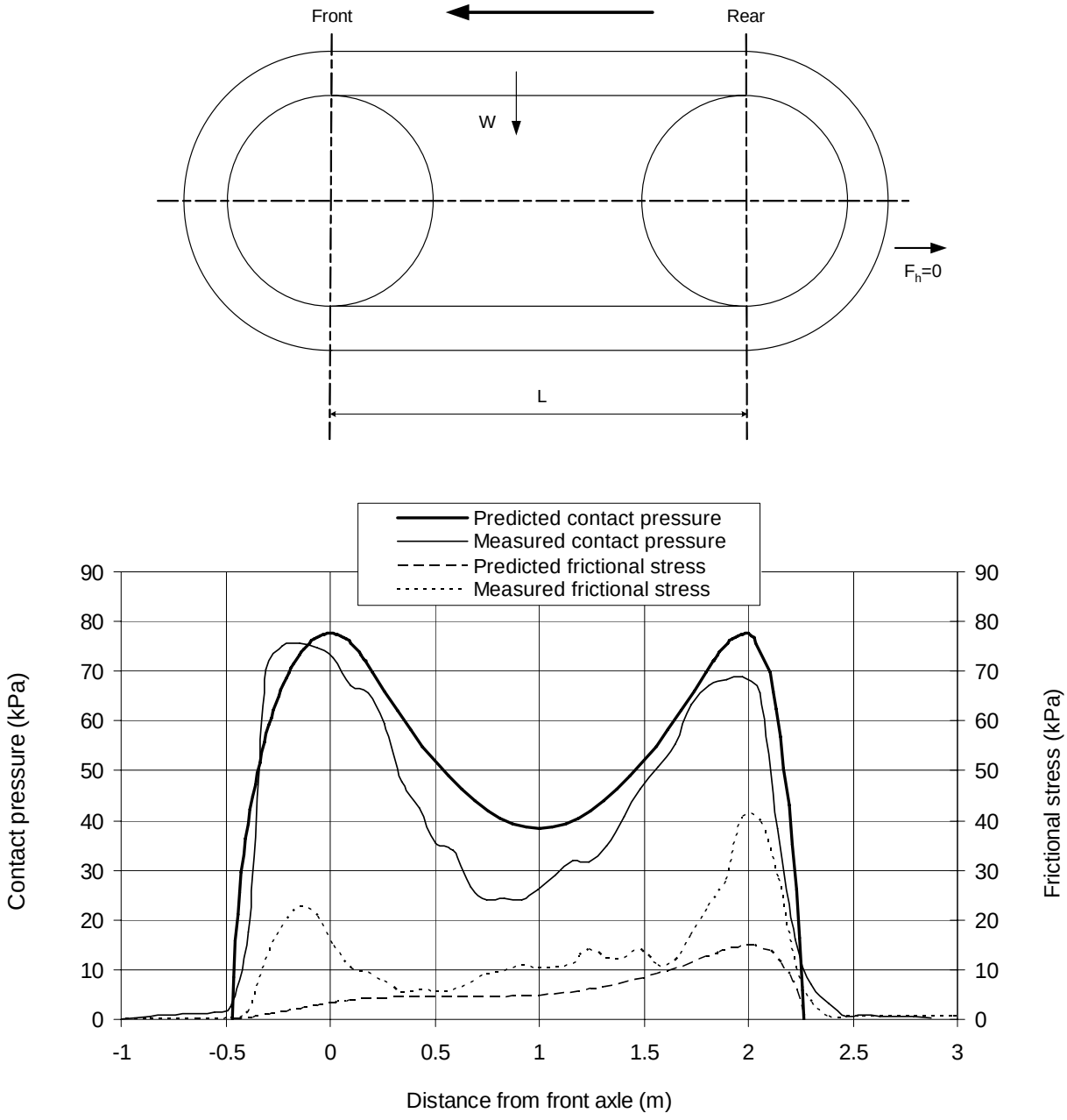

Figure 7.3. The measured and predicted contact pressure distribution and frictional stress on a soft soil surface (drawbar pull = 0, sandy loam soil, soil water content 7.8%).

The tangential stress at any point at the contact surface was calculated by equation (4.2) (p 4-4) after the soil frictional parameters were obtained and the contact pressure determined. The distribution of the tangential stress was predicted.

Based on the measured data the peak value of the contact pressure for the front axle was larger than the value for the rear axle, due to the fact that the centre of gravity of the tractor was longitudinally located in front of the track centre point. When the drawbar pull was zero, the resultant vertical force to support the tractor weight was also located in the same vertical plane running through the centre of gravity. However, for modelling, it was assumed that the front and the rear axles carried equal vertical load before the weight transfer reaches a specified transient level. Based on the model, the peak values of the contact pressure on the front and the rear wheels were therefore predicted as being equal.

The rolling resistance in this case, was measured as 22.8 kN by summing the horizontal force components on the individual track elements. According to the model, the predicted motion resistance based on sinkage was calculated as 9.5 kN which was much lower than the measured value. The contribution probably by internal friction and hysteresis losses was therefore higher than the losses caused by soil compaction and sinkage.

7.2.4 The effect of the ground wheels on the contact pressure distribution and frictional stress for a soft surface

When the ground wheels on the middle of the track were forced down for a soft terrain surface, the measured values of contact pressure distribution and frictional stress is shown in Figure 7.4. The result shows that the contact pressure distribution was more uniform than for a hard terrain surface (Figure 7.2), which proves a possible application for the ground wheels. However, beneath the ground wheels, the contact pressure was still very concentrated, probably due to the fact that the diameter of the ground wheels were relatively small when compared to that of the

drive and the tension wheels. The results, as shown in Figure 7.3 were collected for the tractor with zero drawbar pull.

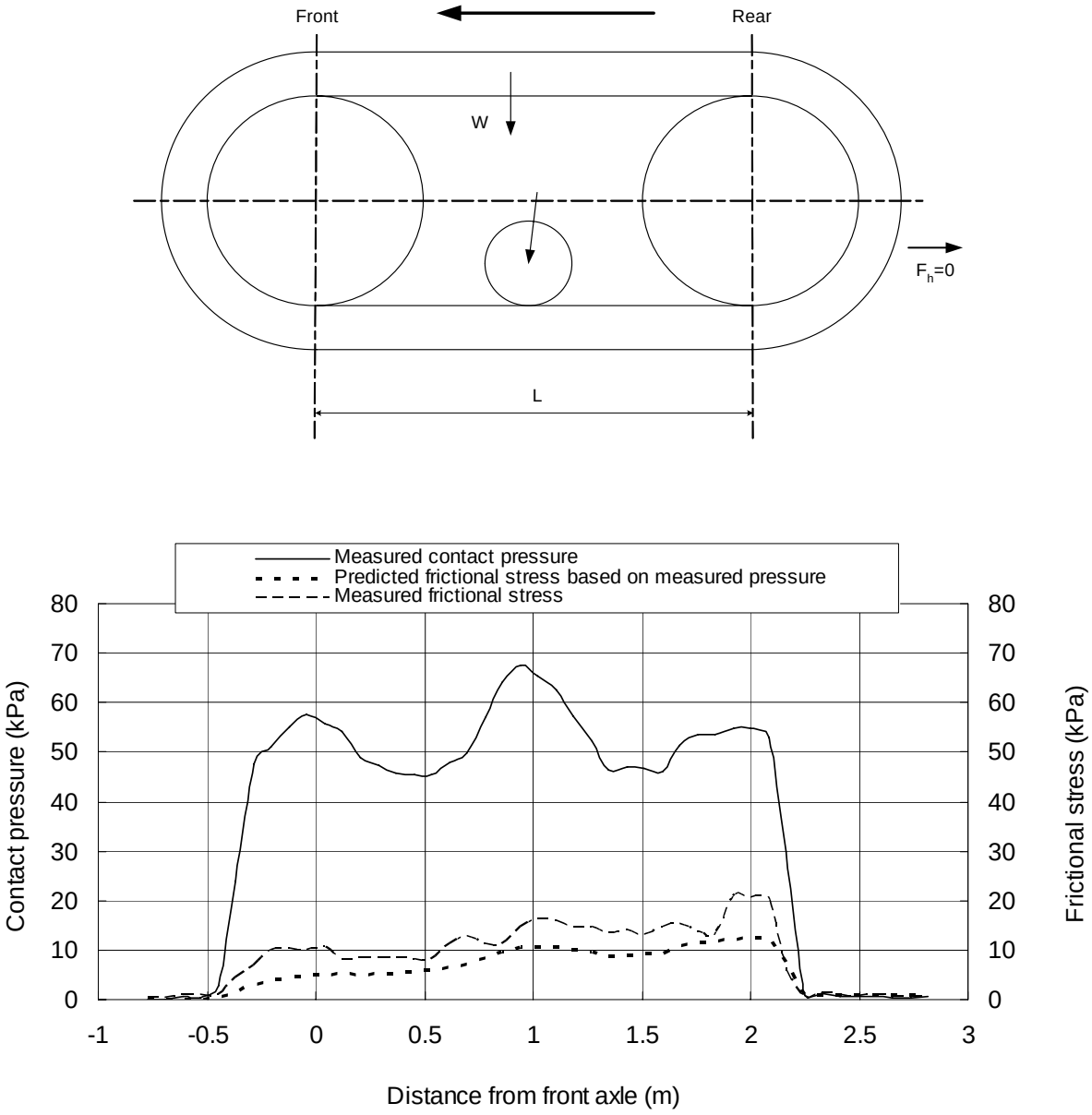

Figure 7.4. The measured contact pressure distribution and frictional stress on soft soil surface when the ground wheels in the middle of the track were pushed down (drawbar pull = 0, sandy loam soil, soil water content 7.8%).

The values for the frictional stresses are very small and mainly represent the thrust to overcome the rolling resistance on the soft terrain surface. However, it was possible to either lift or fully load the centre wheels. However, it again was difficult to achieve a uniform contact pressure below the track during tests by keeping the centre wheel load at a steady level.

Unfortunately, the flexible track model was established to be applicable only under normal operational conditions when the centre ground wheels were lifted. Therefore the predicted contact pressure distribution was not available in this case.

By summation of the measured horizontal force components, a motion resistance of 24.8 kN was obtained which was comparable to the value of 22.8 kN when the centre wheels were not utilized.

7.2.5 The influence of the soil water content and the drawbar pull on the contact pressure distribution

As described in the previous two Chapters, the contact pressure at each point underneath the track was directly related to sinkage, as influenced by the three contact pressure-sinkage parameters, i.e. k_c, k_ϕ, and n obtained from the pressure-sinkage tests. However, the soil water content had an influence on the pressure-sinkage parameters. Typical results from both modelling and experimental measurement of contact pressure and frictional stresses are shown in Figures 7.5 to 7.7. The value of the predicted frictional stresses was calculated by equation (4.2) (p 4-4) based on the predicted contact pressure and the relative slip for the specific point below the track elements. As the slip from front to the rear increased proportionally to the contact distance from the front contact point of the track, the predicted frictional stress and thus friction force on the track element increased at the position closer to the rear.

As shown in the Figures, the predicted contact pressure distribution for soil water content values of 7.8% and 13.3% are very similar in pattern and in peak values.

However, the pressure distribution values for a soil water content of 21% differs from the other two in terms of higher maximum peak contact pressure values (98 kPa vs 78kPa).

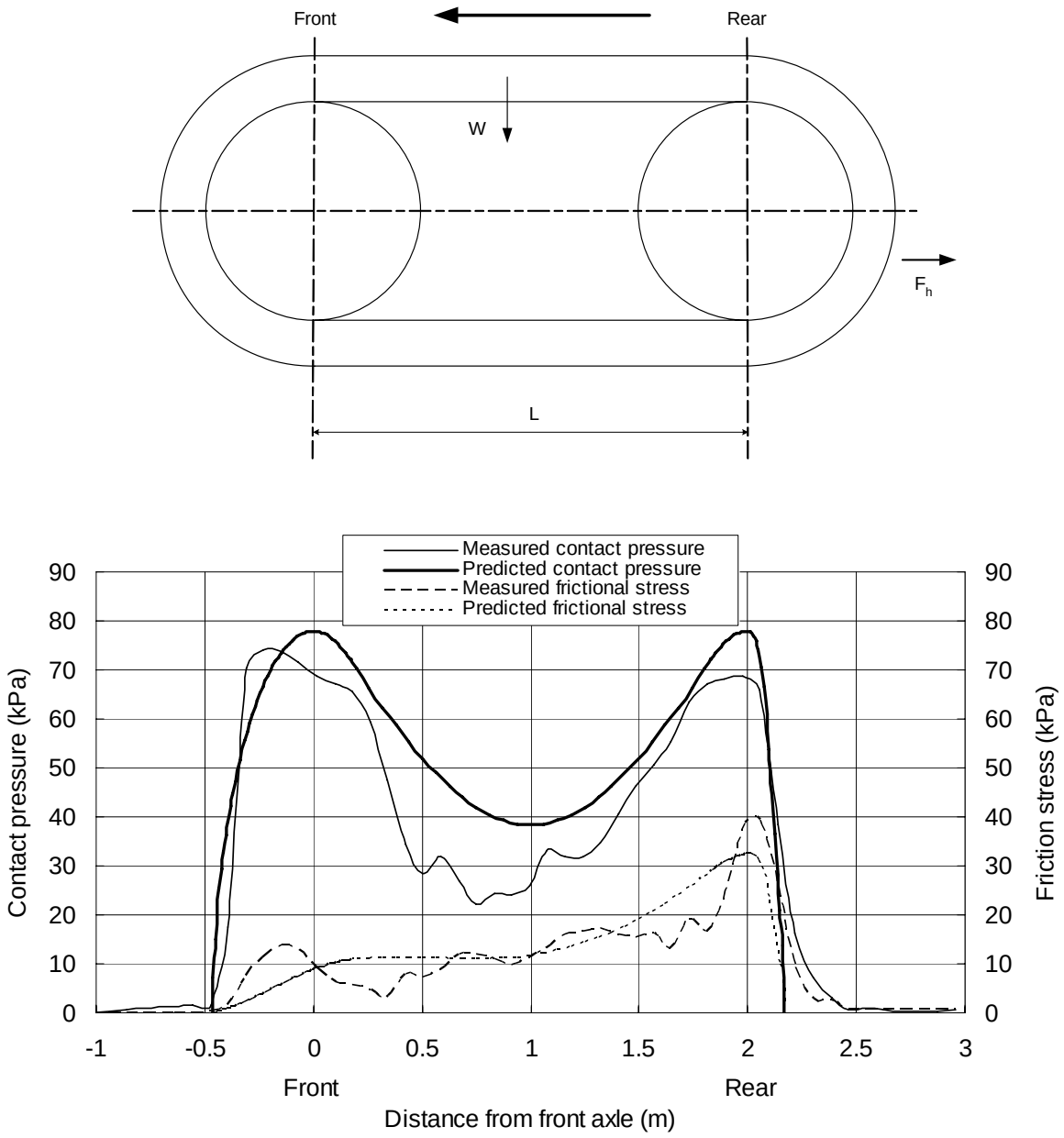

Figure 7.5. The contact pressure and frictional stress distribution for a soil water content of 7.8% (slip=7.2%, drawbar pull=38.7kN, sandy loam soil).

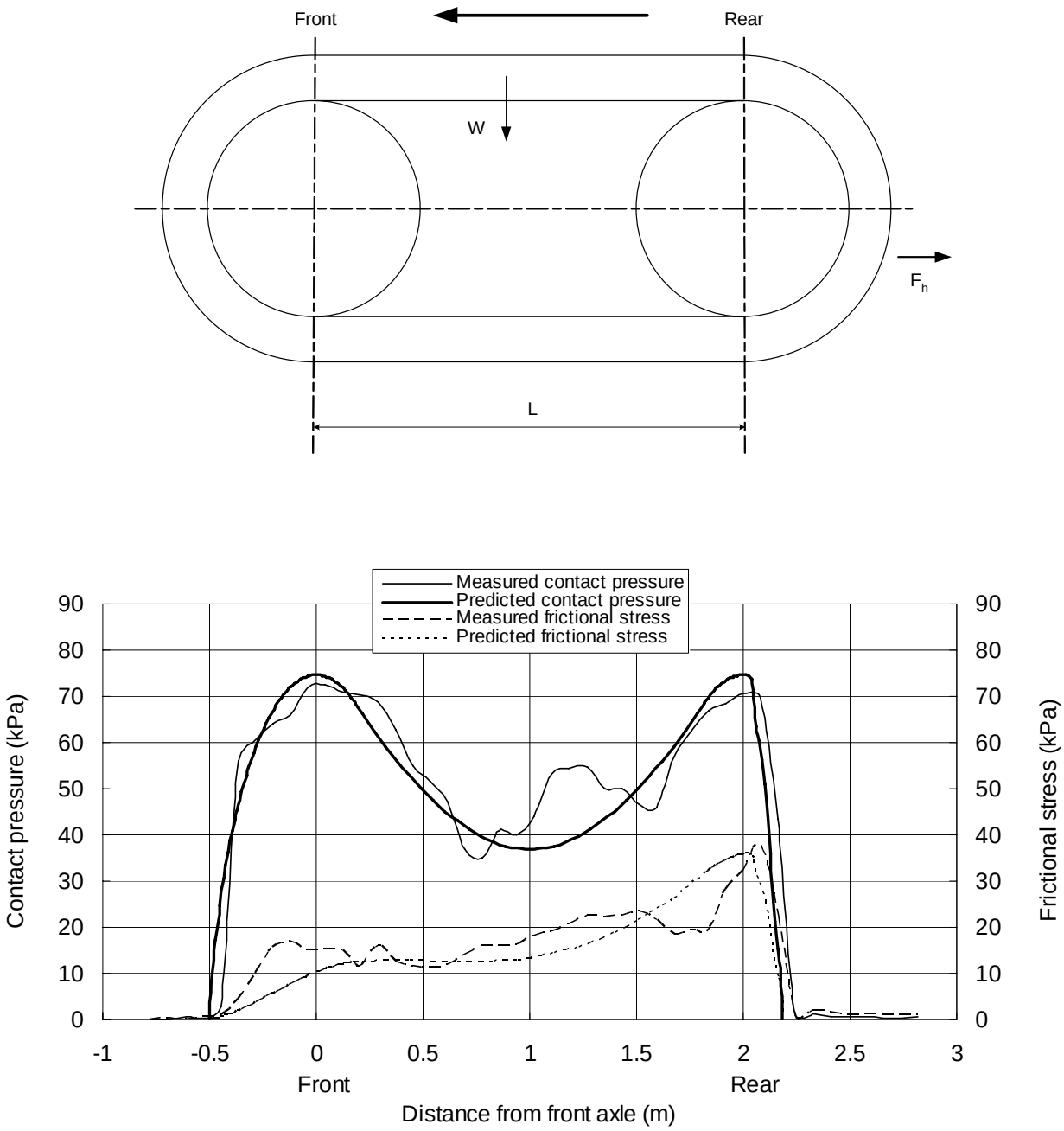

Figure 7.6. The contact pressure and frictional stress distribution for soil water content of 13.3% (slip=7.4%, drawbar pull=41.1kN, sandy loam soil).

As the total tractor mass remained the same during the test, the re-distribution of the contact pressure resulted from weight transfer was caused by different values of drawbar pull. The total vertical load, on the other hand, was kept unchanged. Under these conditions, the predicted and measured contact pressure distribution for a soil

water content value of 21% was less uniform than for the other two soil water content values in terms of the ratios of the minimum contact pressure at the centre of the track to the peak values at both the front and rear wheels.

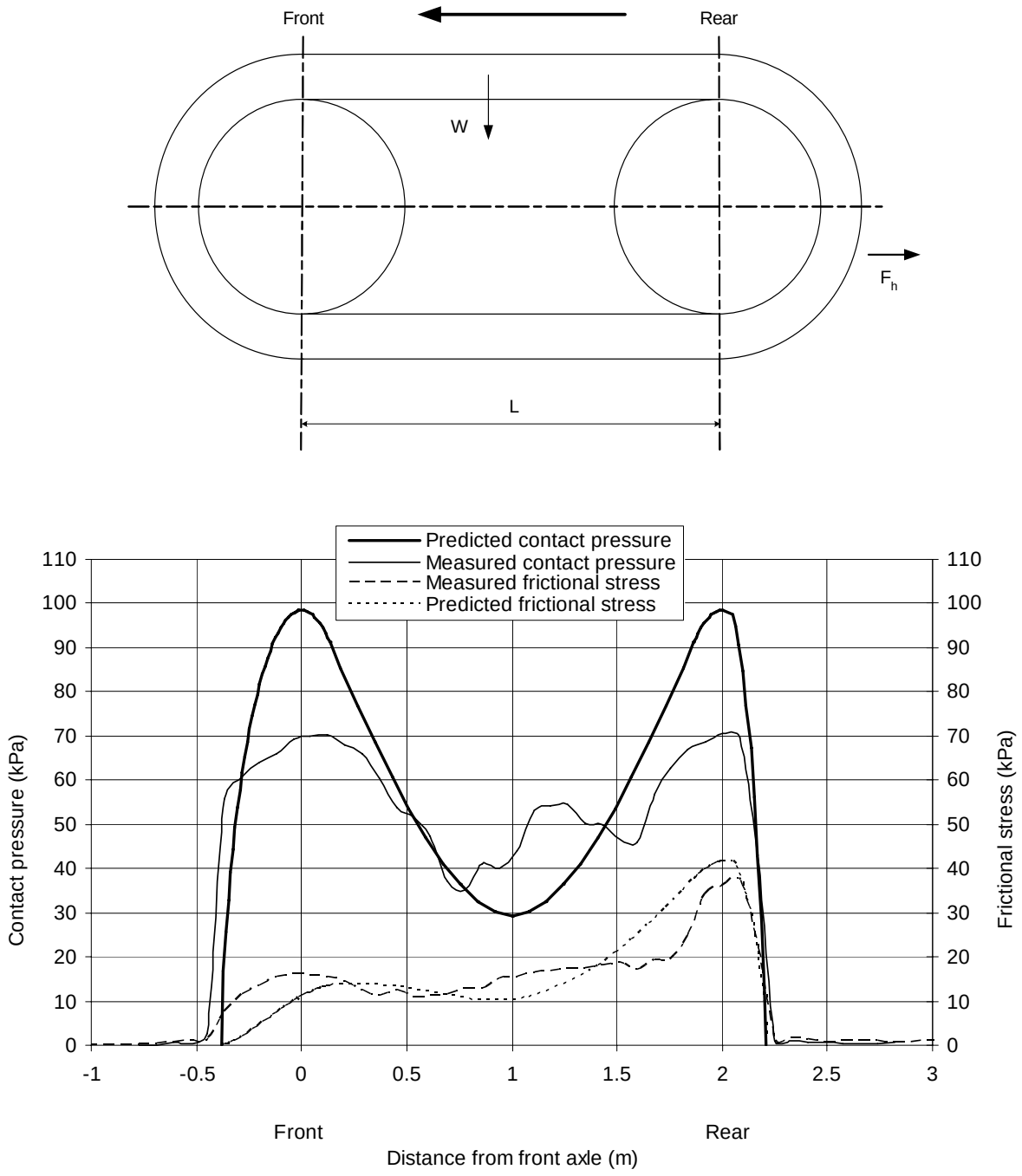

Figure 7.7. The contact pressure and frictional stress distribution for soil water content of 21% (slip=10.4%, drawbar pull=34.9kN, sandy loam soil).

The trend for the curves based on the predicted results in all cases corresponds well with the measured results.

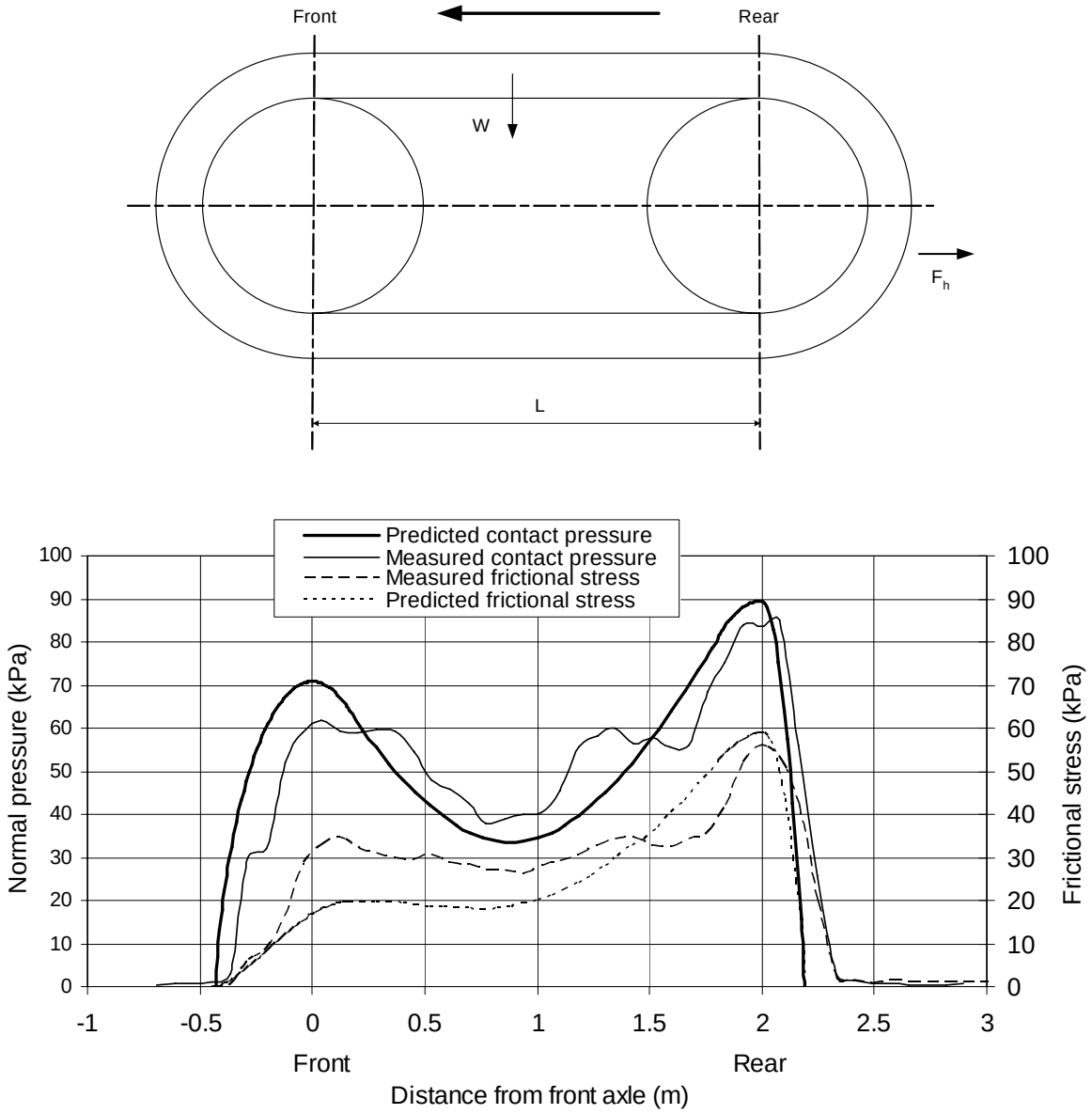

Figure 7.8. The contact pressure and frictional stress distribution for soil water content of 13.3% (slip=12.0%, drawbar pull=57.6kN, sandy loam soil).

Based on the flexible track model, for a drawbar pull of less than a specified value, i.e. 53 kN, the front and the rear wheels had the same contact pressure, thus sinkage values were also similar to the ones as shown in Figure 7.5 through 7.7. When the

drawbar pull was larger than 53 kN, the rear wheels would carry a larger vertical load and thus more sinkage would occur, caused by weight transfer (Figure 7.8). This would be followed by a change in chassis tilt angle.

From Figures 7.5 to 7.8, it can be seen that the flexible track model predicts the contact pressure distribution well for the soil water contents of 7.8% and 13.3%. However, larger differences occur between the maximum and the minimum peak values for the predicted and measured values for a soil water content of 21% (Figure 7.8). The predicted values are still in close correspondence to the measured values for all cases.

It happened during the tests that the soil was very wet for the condition with soil water content 21%. The extreme soil condition possibly caused an extra error for the prediction. The sinkage values for the front and rear wheels of the track were considerably larger than for other soil conditions as observed. The predictions are probably more accurate for soil conditions with low to moderate soil water content values.

7.3 THE RELATIONSHIPS OF TRACTION COEFFICIENT AND TOTAL SLIP

Based on the equations as shown in Chapter 4, the relationship of traction coefficient and slip are shown in Figures 7.9 to 7.10. For comparison purposes, the results for other simplified prediction models are also included in the figures.

In the Figures 7.9 to 7.11, the tractive effort for a specific level of slip was calculated by equations (4.11) (p 4-10) for the idealized distribution model and (4.23) (p 4-16) for the flexible track model when the tangential displacement was related to the slip. The motion resistance was calculated by equation (4.12) (p 4-10) for the idealized distribution model and equations (4.30) (p 4-18) and (4.31) (p 4-19) for the flexible

track model. The coefficients of traction were calculated on the base as defined by equation (4.34) (p 4-22) in Chapter 4.

For the traction coefficients, in all three cases as can be seen from the figures, the results for the uniform distribution model are all over-predicted whilst the results for the flexible model are closer to the measured values. The difference between the predicted and the measured results are probably due to the internal track friction losses. The difference between the coefficients based on the measured torque and rolling radius and the summation of measured tangential stresses also shows a minor influence of some factors which need to be further investigated. Generally speaking, better predicted results were obtained with the flexible model than the uniform contact pressure model.

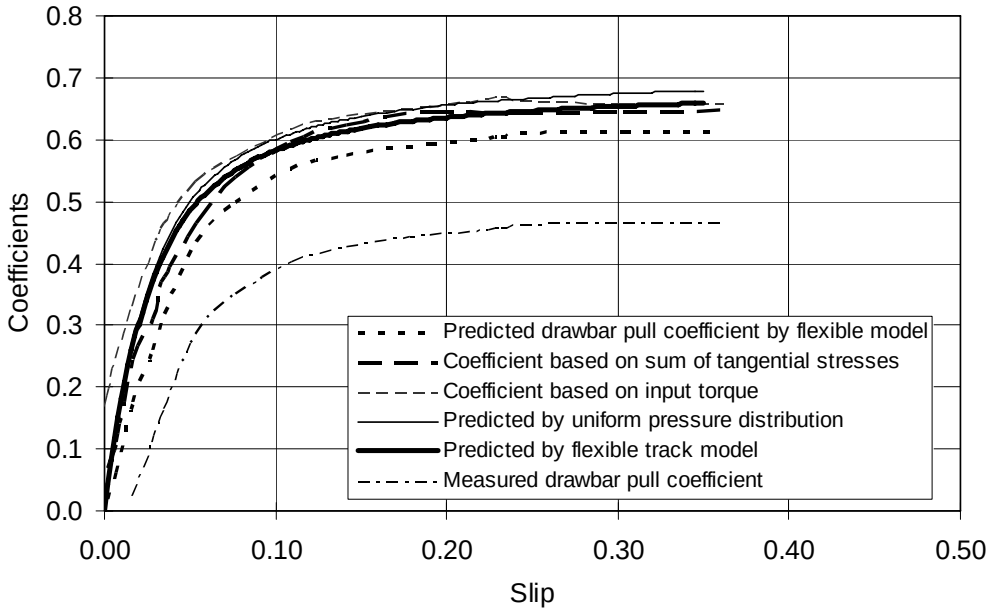

Figure 7.9. The relationship of traction coefficients and drawbar coefficient versus slip for a soil water content of 7.8% (sandy loam soil).

For the drawbar pull coefficient, a large difference exists between the measured drawbar results and the predicted results when the motion resistance is taken into account. It is proved that the internal resistance for such a track is much higher than

the value predicted by conventional modelling methods and needs to be specially investigated.

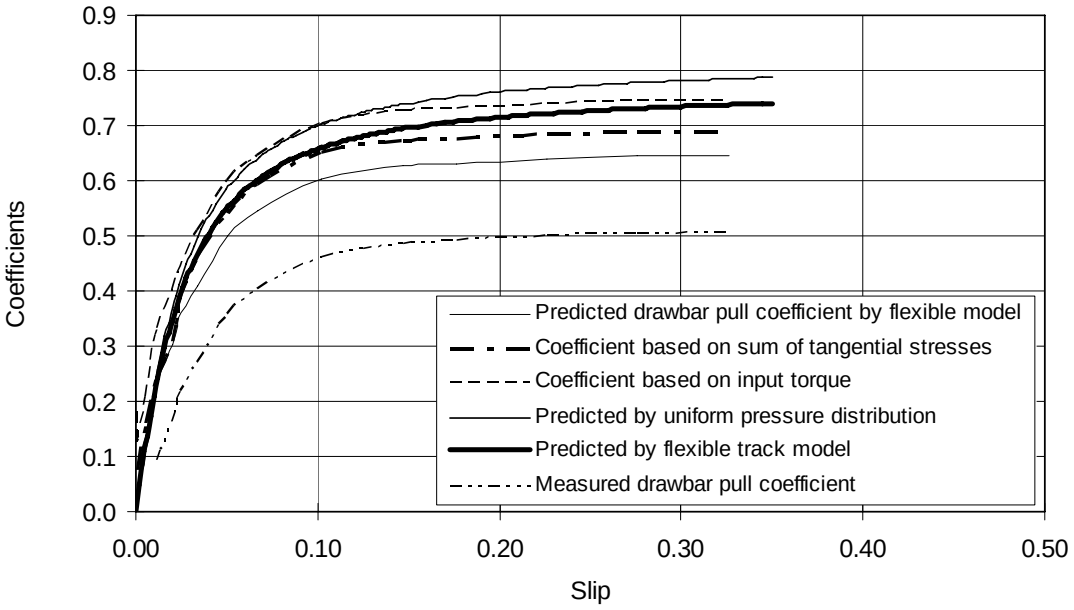

Figure 7.10. The relationship of traction coefficient and drawbar coefficient versus slip for a soil water content of 13.3% (sandy loam soil).

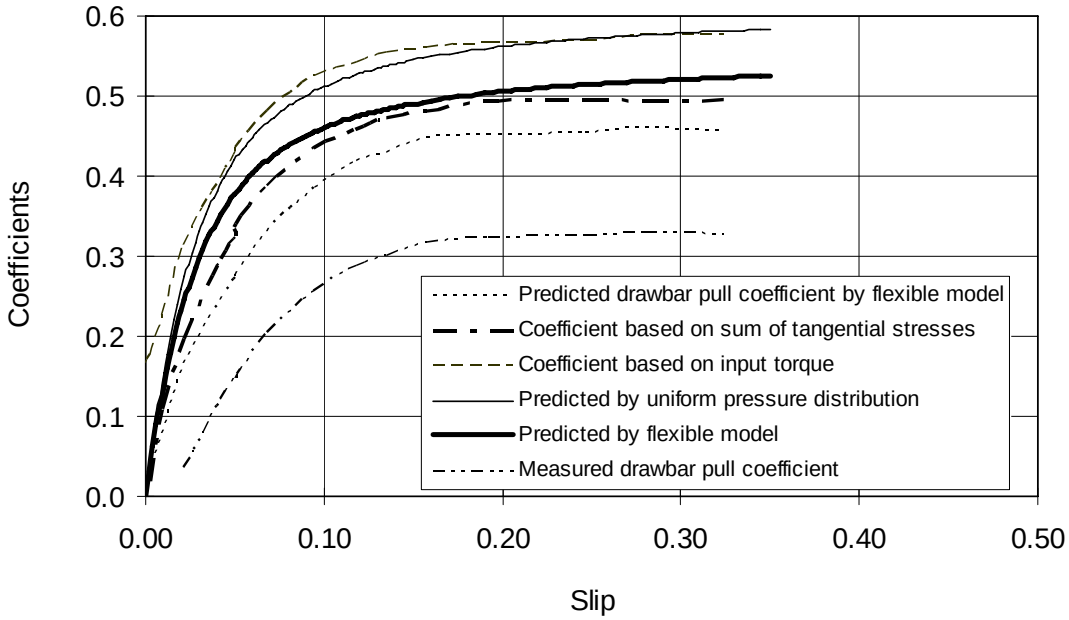

Figure 7.11. The relationship of traction coefficient and drawbar coefficient versus slip for a soil water content of 21% (Sandy loam soil).

It is noticeable that under all three values of soil water content, the predicted results for the model based on the constant contact pressure distribution is closer to the measured results based on the shaft torque, whilst the predicted results for the flexible track model is much closer to the results measured on the base of the summation of tangential stresses.

The results for drawbar pull tests are shown in Appendix A.

From the Figures 7.9 to 7.11, it can be seen that the traction performance is the best for the soil water content of 13.3% whilst it is worst for the 21% soil water content. It is indicated that the soil water content plays an important role influencing the traction performance for the soil with all other conditions unchanged.

For three different soil water content values, the drawbar performance characteristics have different maxima. However, the curves generally exhibit an increase in the traction coefficient with the slip and then approached a constant maximum value for a further increase in slip. This is in accordance with the measured frictional characteristics between the rubber track element and soil.

7.4 THE TRACTIVE EFFICIENCY

As discussed in Chapter 5, the arrangement of strain gauges on the side shaft and the velocity sensors enabled the researcher not only to measure the speeds and to calculate the slip, but also to measure the input torque to the track. It is hence possible to calculate the tractive efficiency η by applying the following equation:

$$\eta = \frac{F_h \times V}{2T\omega} \tag{7.1}$$

where

F_h = drawbar pull, (N).

V = travel speed, (m/s).

T = torque measured on one side shaft, (Nm).

ω = the angular velocity of the shaft, (rad/s).

The tractive efficiencies obtained from the measured test results are shown in Figure 7.12 for all three values of soil water content. For comparison reasons, the predicted tractive efficiencies based on the measured travel speeds are also shown in the figure.

The values of the maximum tractive efficiency obtained under three soil conditions are shown in Table 7.1. The tractive efficiency of the experimental track for low drawbar pull is very low as can be seen from the figure. This is different from the conventional wheeled tractors with a high tractive efficiency for low drawbar pull values. The tendency was probably caused by much higher internal track losses even at low values of drawbar pull.

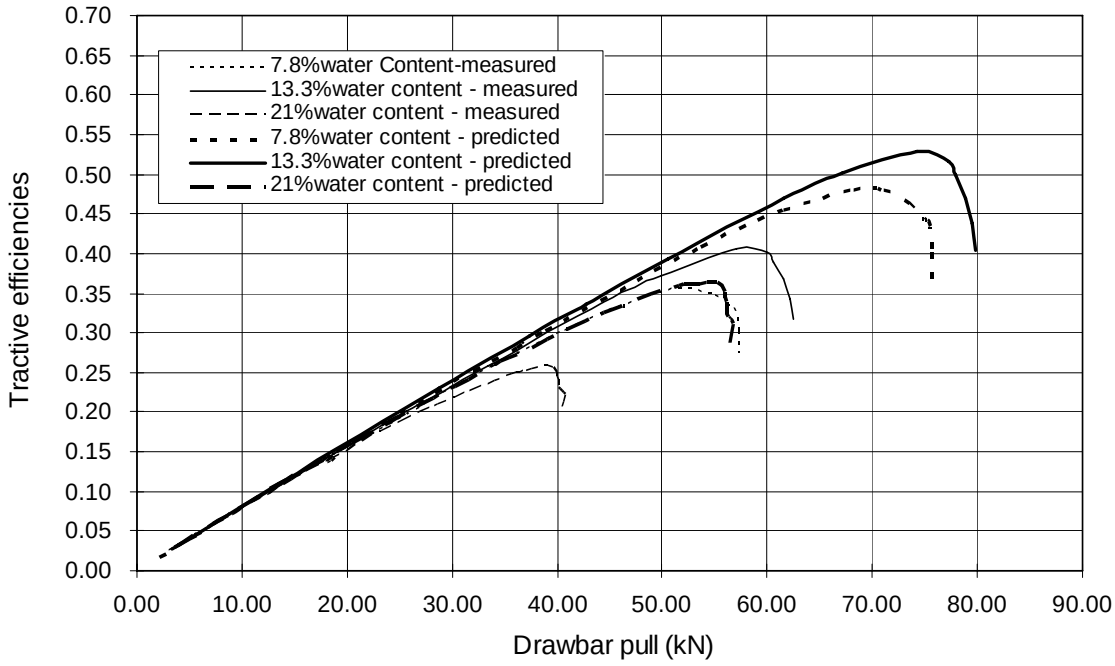

Figure 7.12. Tractive efficiencies from the experimental tests.

Table 7.1. The maximum tractive efficiency.

Soil water content (dry base, %)	7.8	13.3	21
Measured maximum tractive efficiency (%)	35.6	41.8	26.2
Predicted maximum tractive efficiency (%)	48.1	52.8	36.3

7.5 ANALYSIS OF THE FACTORS AFFECTING THE TRACTIVE PERFORMANCE

7.5.1 Soil water content

Under moderate values of soil water content, the tractive performance is the best as shown in the figures and the table. This is probably due to the fact that for a specific soil water content, the combined effect of the rubber-soil friction and adhesion reaches an optimum value when compared to other conditions when the soil is either too dry or too wet. The predicted and the measured results also corresponded well.

7.5.2 Track tension

Track tension is also a very important factor for the frictional drive traction system as it is for a conventional flat belt drive system, especially at high values of drawbar pull. In the preliminary tests, when the track tension was not set to a sufficiently high value, the track did not depict the walking beam effect and excessive slip occurred between the track and the drive wheels at relatively low drawbar pull values. After the track tension was corrected, the friction loss was reduced and the drawbar pull increased.

7.5.3 Motion resistance and internal friction losses

The measured and predicted values of the motion resistances for three soil conditions at different soil water content values are shown in Table 7.2. As can be seen, the predicted and the measured motion resistance values depict large differences probably caused by the internal frictional losses and the friction between the track elements.

Table 7.2. Measured and predicted motion resistances.

Soil type	Soil water content, %, dry basis	Predicted external motion resistance, kN	Measured motion resistance, kN
1	7.8	9.5	22.8
2	13.3	11.7	21.6
3	21	12.6	23.2
4	0, concrete surface	-	12.8

The attention must be drawn to the fact that the measured motion resistance was based on the input torque to the drive shaft and the predicted value by summation of the horizontal force components below the track when the drawbar pull was zero. It is proved that the internal resistance for all conditions was considerably higher than expected.